This paper describes both theoretical and experimental investigations of the error behaviour of cryo current comparators (CCC) as a function of the geometric parameters of the superconducting shields. The basis of our calculations has been the attenuation of magnetic fields by a superconducting coaxial cavity. The theoretical results agree with experiments which have been performed on a special test configuration of a CCC. Its main feature is a toroidal shield made from mercury with an elongated gap region forming the coaxial cavity.

The results obtained are applicable to all types of CCCs. We found that the superconducting coaxial cavity behaves like a filter which transmits only the useful signal containing information about the net current linkage. All other fields contributing to the error of the comparator are attenuated exponentially.

Field attenuation as the underlying principle of cryo current comparators

K. Grohmann, H.D. Hahlbohm, D. Hechtfischer, and H. Lübbig

Since the first reports appeared on cryo current comparators (CCCs)[1,2] and the explanation of the underlying principle[3] using the Maxwell-London equations, several modifications and applications have been described.[4-7] DC errors below 10^{-11} can be obtained compared to values of 10^{-8} for conventional current comparators.

Basically the only difference between various types is their shielding configuration. One model encloses the ratio windings with a superconducting shield which is wrapped around a SQUID magnetometer; while the other encloses a toroidal detection coil by a toroidal shield configuration wrapped by the ratio windings. The detection coil is part of a flux transformer connected to a SQUID magnetometer. Both types may be easily transformed into each other[8] and have been found to be equivalent.

The individual properties of the different types of CCCs are described by solving the Maxwell-London equations taking into account the individual boundary conditions. Because of the complexity of the mathematics analytic solutions of this equation system are limited to special cases.[3] From these results it can be concluded that in the detection area of all CCCs the magnetic field distribution is mainly governed by the superconducting shields and almost completely independent of the positions of the current carrying wires. Furthermore, experiments with the toroidal configurations show that the error behaviour depends on the geometric parameters of the shield.[8] This suggests that field components which do not contain information about the net current linkage are attenuated on the way from the ratio windings to the detection area. This assumption of field attenuation gives a promising starting point for a detailed description of the influence of geometric parameters on the error of CCCs without requiring a complete solution of the Maxwell-London equation system.

The authors are with the Physikalisch-Technische Bundesanstalt, Institut Berlin, 1 Berlin 10, Abbestr 2-12, Germany. Received 13 January 1976.

In this paper we aim to elaborate this approach theoretically and experimentally for the geometry of a double cylinder arrangement. As will be discussed later, this geometry is common to all known CCCs if the outer shielding is considered part of the comparator system. In the first part of this paper the field attenuation in a double cylinder is analytically developed and numerically calculated for some relevant cases. In the second part experiments are described whose results are in agreement with the calculations and confirm the attenuation model of the CCCs.

Theory

Foundation of the diamagnetic model

Considering shields consisting of superconductors of the London type. Disregarding non-local effects this means that the relation between the spatial density $\mathbf{j}^{(s)}$ of the superconducting screening currents and the electromagnetic fields **E**, **B** are given by

$$\mu_0\lambda^2 \nabla \times \mathbf{j}^{(s)} = -\mathbf{B} \qquad \mu_0\lambda^2 \frac{\partial}{\partial t}\mathbf{j}^{(s)} = \mathbf{E} \qquad (1)$$

Here λ denotes the temperature-dependent penetration depth and μ_0 is the permeability of vacuum. The distribution of the electromagnetic field is governed in a unique way by the Maxwell theory, supplemented by the proper boundary conditions.

For the case of a superconducting shield surrounding a current carrying wire, the exponential decay of the penetrating field due to the Meissner effect is accompanied by a strong deformation of the field pattern. The magnetic field lines tend to adapt themselves to the contours of the superconducting shield.[3] If the thickness of the shield is large compared with the penetration depth, the field distribution in the outer domain practically equals that caused by an

ideal diamagnetic shield configuration. In this diamagnetic representation the magnetic field is completely excluded from the interior of the shielding material and the response to an applied field is given by surface currents of density $g = \lim_{\lambda \to 0} (\lambda j^{(s)})$.

In the following we use the Maxwell-London theory in this ideal diamagnetic limit. Furthermore, we assume that superconductivity has been set up without any magnetic field, that is, frozen-in-fluxes are neglected. If we confine our considerations to stationary cases we can derive the magnetic field outside the superconductor from a scalar potential V

$$\mathbf{B} = -\nabla V \tag{2}$$

which obeys the Laplace equation

$$\Delta V = 0 \tag{3}$$

The diamagnetism of the superconducting shields is described by

$$\frac{\partial V}{\partial n} = 0 \tag{4}$$

on all shield surfaces where $\partial/\partial n$ denotes the derivation with respect to the normal of the surface.

Field attenuation by concentric superconducting cylinders

The arrangement considered is shown in Fig. 1. A cylindrical cavity of inner radius r_i, outer radius r_a, and of infinite depth is formed by two concentric cylinders. Outside the cavity a magnetic field exists, whose penetration into the cavity will be studied.

In cylindrical coordinates the Laplace equation is given by

$$\frac{1}{\rho}\frac{\partial}{\partial \rho}\left(\rho \frac{\partial V}{\partial \rho}\right) + \frac{1}{\rho^2}\frac{\partial^2 V}{\partial \phi^2} + \frac{\partial^2 V}{\partial z^2} = 0 \tag{5}$$

Using $V(\rho, \phi, z) = R(\rho)\,\Phi(\phi)\,Z(z)$ (5) can be split up into three ordinary differential equations of second order, the solutions of which are connected by two separation parameters n and k[9]

$$\Phi(\phi) = \begin{cases} A\phi + B & n = 0 \quad (6a) \\ A_n \sin(n\phi + \theta_n) & n > 0 \quad (6b) \end{cases}$$

$$Z(z) = \begin{cases} Cz + D & k = 0 \quad (7a) \\ C_k e^{+kz} + D_k e^{-kz} & k > 0 \quad (7b) \end{cases}$$

$$R(\rho) = \begin{cases} E \ln \rho + F & n = 0 \quad k = 0 \quad (8a) \\ E_n^0 \rho^n + F_n^0 \rho^{-n} & n > 0 \quad k = 0 \quad (8b) \\ E_n J_n(k\rho) + F_n Y_n(k\rho) & n \geq 0 \quad k > 0 \quad (8c) \end{cases}$$

where J_n and Y_n denote ordinary Bessel functions of the first and second kind, respectively and of integer order.

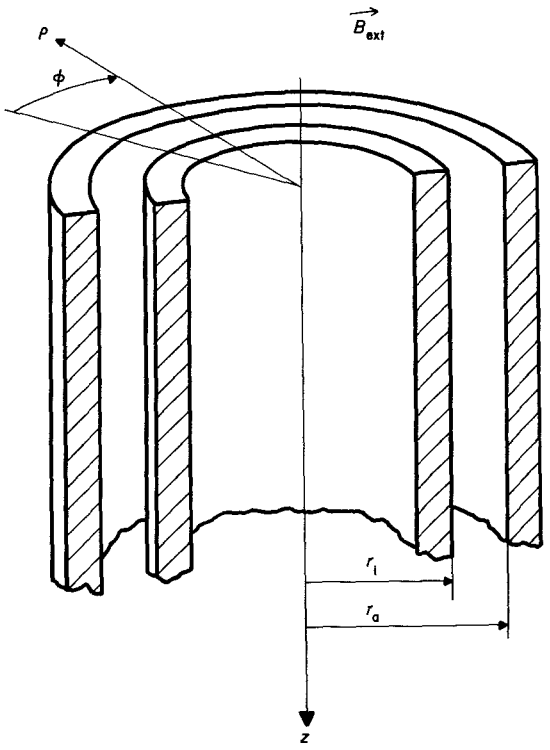

Fig. 1 Coaxial cavity

The general solution for V is obtained by summing up the combinations of R, Φ, and Z for all possible values of n and k. These values must be determined together with the coefficients $A \cdots F$ from the boundary conditions:

The symmetry of the external field **B** determines the symmetry of our solution and thus the related values of n. If V is to be single-valued, we get $A = 0$. If we allow an axial current I to flow in the region $\rho < r_i$ from Ampere's law $A = -\mu_0 I/2\pi$. Because of the infinite depth of the cavity and the exclusion of a frozen-in field we further obtain $C = C_k = 0$. The last boundary condition

$$\frac{\partial V}{\partial n} = 0 \quad \text{at} \quad \rho = r_i \quad \text{and} \quad \rho = r_a \tag{9}$$

leads to $E = E_n^0 = F_n^0 = 0$.

The complete solution in our case is given by

$$V(\rho, \phi, z) = -(\mu_0 I/2\pi)\phi + \sum_{\text{all } k} A_{0k}[E_0 J_0(k\rho) + F_0 Y_0(k\rho)]\, e^{-kz} + \sum_{n=1}^{\infty} \sum_{\text{all } k} A_{nk}[E_n J_n(k\rho) + F_n Y_n(k\rho)] \sin(n\phi + \theta_n)\, e^{-kz} \tag{10}$$

As we are interested in the attenuation of the applied field with increasing z, we have to determine the values which

the constant k can assume. The boundary conditions (9) lead to

$$E_n J_n'(kr_i) + F_n Y_n'(kr_i) = 0$$
$$E_n J_n'(kr_a) + F_n Y_n'(kr_a) = 0 \qquad (11)$$

where the prime denotes the derivative $\partial/\partial\rho$. To ensure unique solutions E_n and F_n the determinant has to vanish

$$J_n'(kr_i)\, Y_n'(kr_3) - J_n'(kr_a)\, Y_n'(kr_i) = 0 \qquad (12)$$

This eigenvalue equation has an infinite number of solutions, which determine the possible values of k. These solutions can be found in the literature for a variety of r_a/r_i ratios[10]. Each order n has its own set of solutions $k_1^n, \ldots, k_m^n, \ldots$ Therefore fields of different symmetry, that is different n, will be attenuated in a different manner. This analysis shows that the field attenuation in the coaxial cavity is determined by the solutions of the eigenvalue problem. The important cases are considered quantitatively in the following sections.

Fields of first order ($n = 1$)

The external applied field is assumed to have a potential

$$V_{ext}(\rho, \phi, z) = \overline{V}(\rho, z) \sin\phi$$

This can be realized by a homogeneous field, $\overline{V} = \text{const}\ \rho$, or by a magnetic dipole at $\rho = 0$, $\overline{V} = \text{const}\ \rho/(\rho^2 + z^2)^{3/2}$. For this symmetry (10) reduces to

$$V(\rho, \phi, z) = \sum_{m=1}^{\infty} V_m(\rho, \phi)\, e^{-k_m^1 z} \qquad (13)$$

The first three roots[10] of the eigenvalue equation (12) for this case are plotted in Fig. 2 as a function of the ratio r_a/r_i. For a very thin cavity, that is $r_a/r_i \to 1$, only one root $k_1^1\, r_a = 1$ exists, giving

$$V(\rho, \phi, z) = V_1(\rho, \phi)\, e^{-1z/r_a} \qquad (14)$$

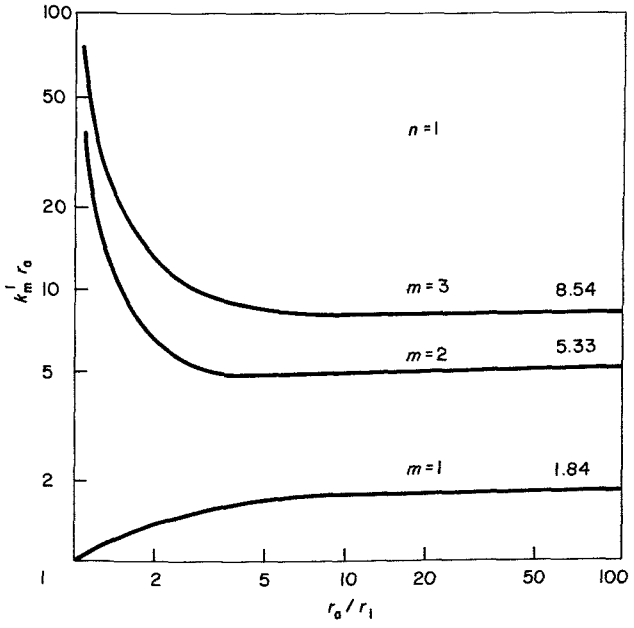

Fig. 2 The first three roots $k_m^1\, r_a$ of

$$J_1(k_m^1 r_i)\, Y_1'(k_m^1 r_a) - J_1'(k_m^1 r_a)\, Y_1'(k_m^1 r_i) = 0$$

For a somewhat broader cavity we obtain finite contributions from the higher roots, for example, for $r_a/r_i = 1.1$

$$V = V_1 e^{-1.05 z/r_a} + V_2 e^{-34.5 z/r_a} + V_3 e^{-69.1 z/r_a} + \ldots \qquad (15)$$

Because of the rapid decreases of the exponentials only the first term gives any noticeable contribution. For the limit $r_i \to 0$, that is the cavity becoming a simple tube, we find from Fig. 2 the known result[11]

$$V = V_1 e^{-1.84 z/r_a} + \ldots \qquad (16)$$

This shows the simple superconducting tube is more effective in attenuating transverse magnetic fields than a coaxial type cavity.

Fields of higher order ($n > 1$)

The potential of the external applied field may contain all sinusoidal components

$$V_{ext}(\rho, \phi, z) = \sum_{n=1}^{\infty} \overline{V}_n(\rho, z) \sin(n\phi + \theta_n) \qquad (17)$$

This type of potential corresponds in general to an inhomogeneous field. In the proceeding section only the first eigenvalue ($m = 1$) gave a measurable contribution. Here this is also valid. If we consider for each order n only the first eigenvalue, then the double sum of (10) reduces to

$$V(\rho, \phi, z) = \sum_{n=1}^{\infty} V_n(\rho, \phi)\, e^{-k_1^n z} \qquad (18)$$

As can be seen from Fig. 3 this sum is given in the case of a very thin cavity by

$$V = V_1 e^{-1z/r_a} + V_2 e^{-2z/r_a} + V_3 e^{-3z/r_a} + \ldots \qquad (19)$$

From this we see that terms of nth order will display n times stronger attenuation than the first order contributions. Therefore, we expect these higher modes to be measurable only at shorter screening lengths, that is, for $z/r_a < 2$. At larger values of z the longest remaining term, if still measurable, will be the first one.

Field of order zero ($n = 0$)

The applied field is taken as axially directed and independent of ϕ. Now we must select from (10) all solutions with $n = 0$, that is

$$V(\rho, z) = \sum_{m=1}^{\infty} V_m(\rho)\, e^{-k_m^0 z} \qquad (20)$$

The first three eigenvalues[10] of the corresponding zero-order eigenvalue equation are plotted in Fig. 4. For a thin cavity we have very strong field attenuation. Even in the limit $r_a/r_i \to \infty$ (simple cylinder) the known[11] result

$$V = V_1 e^{-3.83 z/r_a} + \ldots \qquad (21)$$

gives an attenuation stronger than that of transverse fields. We may therefore omit axially directed fields from further considerations.

Field of a current carrying wire

We are interested in the attenuation of the field which is generated by a current I flowing in axial direction at $\rho = \epsilon\ (0 \leqslant \epsilon < r_i)$ and $\phi = 0$. It can be shown that the potential of this current in a plane above the cavity is given by

$$V_{ext}\ (\rho, \phi)$$

$$= -\ (\mu_0 I/2\pi)\ \left[\phi + \sum_{n=1}^{\infty} n^{-1} \left(\frac{\epsilon}{\rho}\right)^n \sin n\,\phi\right] \quad (22)$$

From the proceeding paragraphs we know that the terms in the sum containing the position ϵ of the current are attenuated exponentially. On the other hand, as can be seen by studying (10), the remaining term $(-\mu_0 I/2\pi)\phi$ is the only solution which exists within the cavity without any attenuation. Besides this it contains no information about the position of the current. To obtain information about the current independent of its location is essential for an ideal current comparator.[3] We see that the coaxial cavity approaches this ideal comparator at a depth z where the ϵ-dependent terms are negligible.

Miscellaneous

There are two points we still have to consider. First, what changes occur when we limit the depth of the cavity to a finite value? In this case the positive exponential in (7b) must also be taken into account. The new boundary condition

$$\frac{\partial V}{\partial z} = 0 \quad \text{at} \quad z = l \quad (23)$$

determines the ratio of the coefficients, giving

$$Z(z) = D_k(e^{-2kl}e^{+kz} + e^{-kz}) \quad (24)$$

This expression only deviates noticeably from the former solution e^{-kz} near the bottom with a maximum deviation factor of two.

The second factor requiring clarification is the optimal values of the radii r_a and r_i in a real comparator. Since $1/r_a$ occurs in the exponentials, for fixed ratio r_a/r_i smaller radii will give stronger attenuation. Taking the smallest value for r_i, normally determined by the space necessary to bring up the ratio-windings, the best attenuation is obtained for $r_a \approx r_i = r_{min}$. This can be observed by dividing the roots of (12) by the ratio r_a/r_i, choosing the inner radius r_i as a reference in this way.

For small values of the width d of the cavity, $d = r_a - r_i < 0.2\, r_i$ the values of $k_1^1\, r_a$ plotted in Fig. 2 can be approximated by

$$k_1^1\, r_a \approx 1 + \frac{d}{2r_i} \quad (25)$$

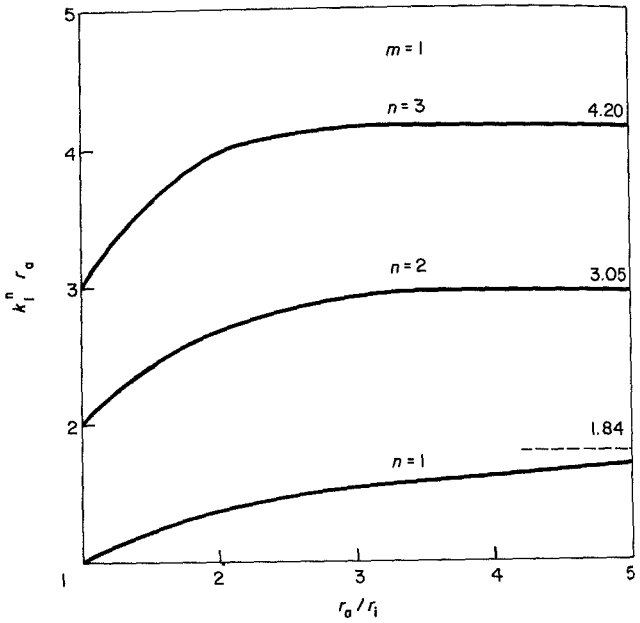

Fig. 3 The first root $k_1^n\, r_a$ of

$$J_n'(k_1^n r_i)\, Y_n'(k_1^n r_a) - J_n'(k_1^n r_a)\, Y_n'(k_1^n r_i) = 0$$

for $n = 1, 2, 3$

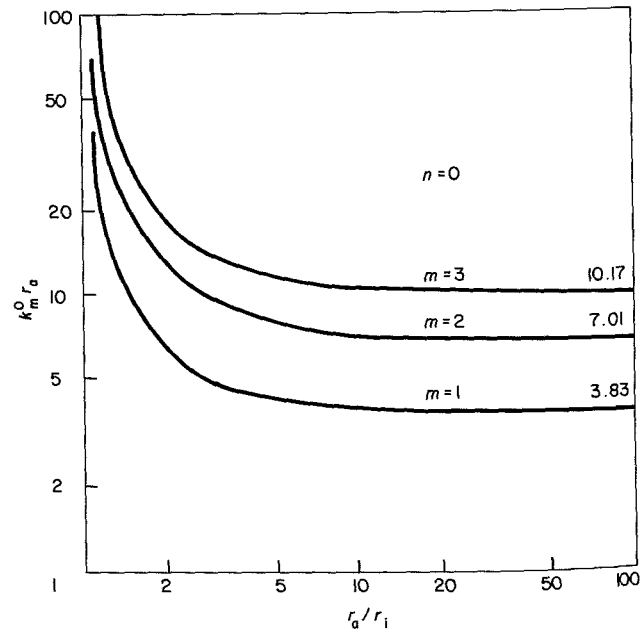

Fig. 4 The first three roots $k_m^0\, r_a$ of

$$J_0'(k_m^0 r_i)\, Y_0'(k_m^0 r_a) - J_0'(k_m^0 r_a)\, Y_0'(k_m^0 r_i) = 0$$

This demonstrates that in the case of thin cavities the attenuation is nearly independent of the width.

By evaluating the complete solution (10), the same can be shown for the field-strength itself. Since in real comparators part of the flux leaving the gap region and entering the detection coil is measured, we may expect therefore the error signal of a CCC to be proportional to the width of the cavity.

Experimental details

Apparatus and method

The experiments were carried out using specially constructed CCCs of the toroidal type (Fig. 5) with mercury superconducting shields ($T_c = 4.15$ K). As mercury is in the liquid state at room temperature, it allows the length l of the superconducting shields simply to be altered by adding a suitable amount of mercury. Using plastic foils to separate the mercury in the gap region we obtain very thin and uniform gaps of well-defined thickness. The cylindric plastic foils are cemented on top of the detection coil, which is sealed with adhesive to protect it against mercury. The detection coil is fixed in position by several niobium screws. The data of the two comparators used were:

	A	*B*
Total height	150 mm	160 mm
Max shield length	110 mm	125 mm
Diameter of foil cylinder	65 mm	34 mm
Thickness of foil	25/50/100 μm	50 μm
Turn number of ratio windings	20	20
Ratio	1/1	1/1

The error E of the CCC is defined by

$$\frac{I_1}{I_2} = \frac{N_2}{N_1}(1 - E)$$

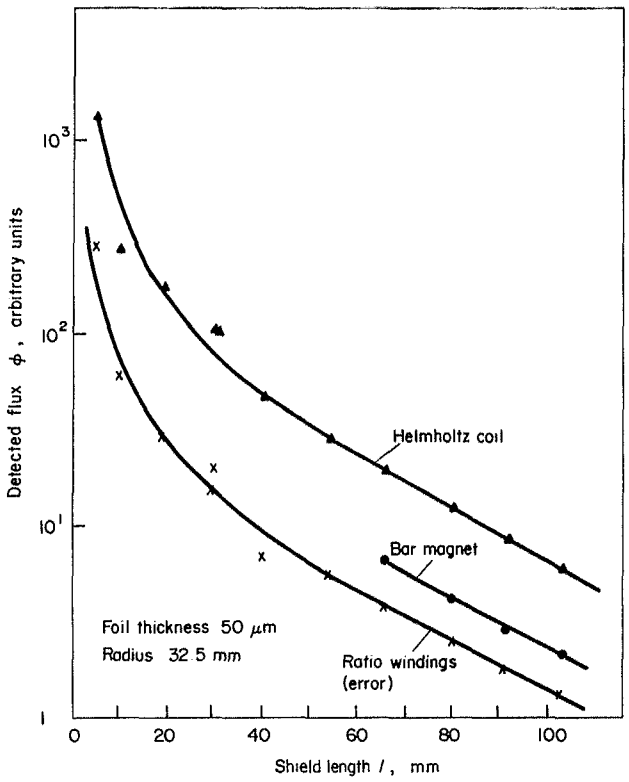

Fig. 6 Attenuation of different magnetic fields as a function of the shield length. (The linear parts correspond to a decay length of 31 mm. The curves are arbitrarily shifted in vertical direction.)

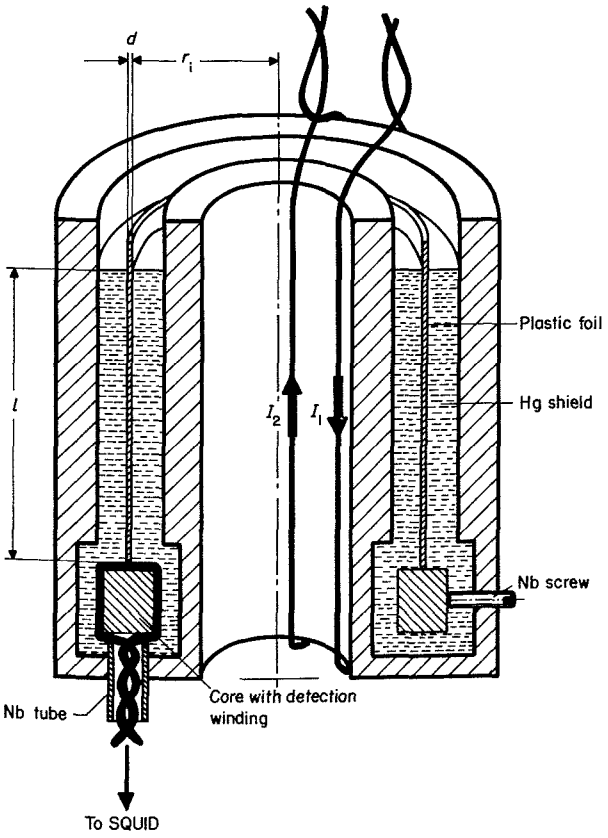

Fig. 5 Cryo current comparator with variable shield length

as the deviation of the current ratio from the ratio of the turn numbers, if the detector indicates zero. The primary and secondary windings of the comparator have been displaced by 180°. By this the zero error, that is, the error without any shield, becomes insensitive to accidental variations of the individual turn positions.

Each of the shield configurations has been exposed to three different fields, different in respect to their origins and their distributions.

1. The field of a pair of Helmholtz coils placed outside the cryostat and representing a nearly homogeneous field normal to the axis of the cylinder.
2. The field of a small bar magnet outside the cryostat and representing an inhomogeneous field.
3. The field generated by the ratio windings with opposite current direction to obtain vanishing current linkage. With this field the error of the different CCCs has been determined.

The detection winding was connected to an rf SQUID-magnetometer as part of a flux transformer. The resulting flux due to the exposition to the three different fields has been registered with a reproducibility of a few percent.

Results

In Fig. 6 the variation of the SQUID signal with varying length is shown for the three different magnetic fields. The width of the cavity was 50 μm, giving a ratio r_a/r_i which deviates from one by only 1.5×10^{-3}. This means that we

must compare the results with the calculations in the limit $r_a \approx r_i$.

From Fig. 6 it can be seen that:

(a) Regardless of their different origin and configuration the three probing fields produce the same exponential decay with increasing screening length for lengths greater than about 60 mm. The measured decay length (decay by factor of e) is (31 ± 2) mm. The calculated value is 32.5 mm.

(b) The faster decay at shorter screening lengths confirms the prediction concerning the detectability of the higher modes for inhomogeneous fields, the decay lengths of which have been shown to be $r_a/2$, $r_a/3$ etc. (The terms of higher order in the case of the Helmholtz coils can be explained by field distortion caused by other superconducting materials nearby.)

In Fig. 7 the attenuation of external fields with varying screening length is shown for three different widths of the coaxial cavity: 25 μm, 50 μm, and 100 μm. (By measurement of the capacity it was shown that the thickness of the foils used really determines the width of the annular cavity.) The measurements show that the attenuation is independent of the width of the cavity for the foils investigated. The theoretical prediction is that the decay lengths deviate from the radius of the cylinder for the three foils investigated by only 0.7×10^{-3}, 1.5×10^{-3}, and 3×10^{-3}, respectively. These small deviations cannot be resolved in our experiments.

For two of the three foils the absolute flux values could also be compared as they were glued to the same detector coil. Small random deviations from circular symmetry in the wiring of the detector coil determine the flux deflexion measured by the SQUID. Therefore absolute comparisons of fluxes intruding in different annular widths may be gained

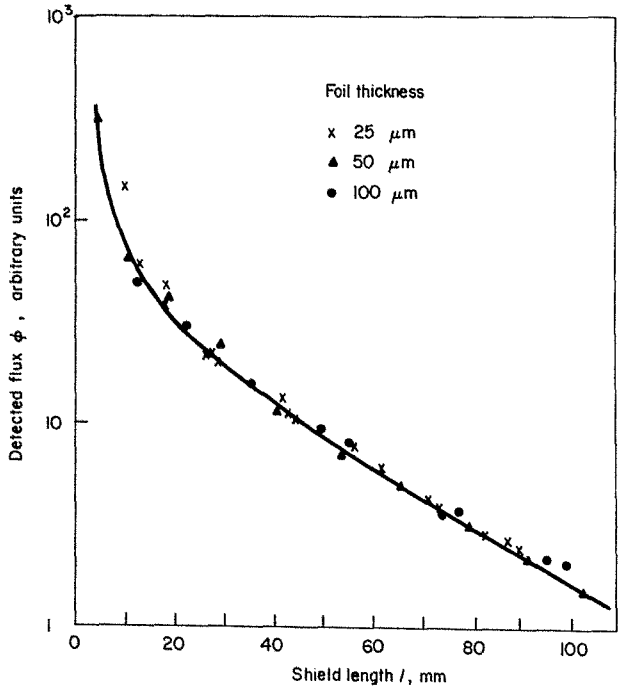

Fig. 7 Attenuation of external fields for three different values of foil thickness as a function of the shield length. (The results for each thickness have been shifted in the vertical to show the common law.)

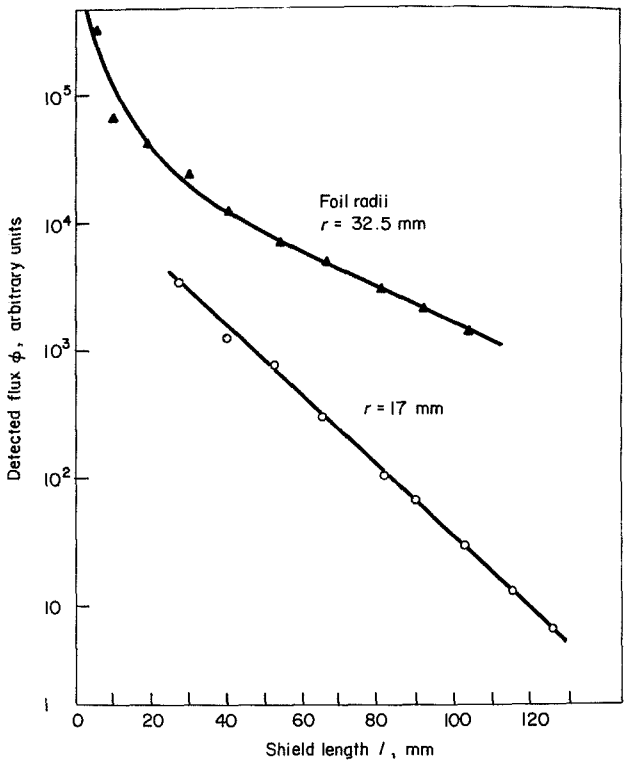

Fig. 8 Attenuation of external fields for different foil radii as a function of shield length. (The decay lengths determined from this figure are 31 mm and 16 mm respectively.)

only by using the same detector coil. With the same shield length we found within experimental accuracy a linear relationship between flux registered and foil thickness. A practical consequence for the design of a CCC is to obtain increasing shield length – which is easier to realize – in preference to decreasing slit width.

Fig. 8 demonstrates the increasing attenuation of external fields with decreasing radius. The decay length measured with the second comparator is (16 ± 1.5) mm which is in good agreement with the theoretical prediction of 17 mm. This result confirms the radius of the coaxial-type cavity to be a very important design parameter.

In an additional experiment we investigated the effect of an axially directed field. We could not observe any signal, which agrees with theory. The experimental results point out that for all practically occuring field distributions, the contribution of the field component associated with k_1^1 governs the field attenuation within the cavity of a cryo current comparator and thus the shield dependent error behaviour.

Summary

The theoretical results of the attenuation model which have been verified experimentally can be summarized as follows.

The coaxial cavity exponentially attenuates any field not contributing to the net current-linkage. Only these fields contribute to the error of the comparator. This error essentially depends on the radius r, length l, and width d of the coaxial cavity according to

$$E \sim d\, e^{-l/r}$$

This means that each screening length of 2.3 radii reduces the error by one order of magnitude.

For comparators with very small errors a single cavity could give an inconvenient total height. This can be avoided by folding the slit region, which is possible using a variety of methods.[8] This causes a new rim-like transverse cavity element to appear, the attenuation of which is negligible in many cases.[12] The most effective folding is a meander-like one at the inner radius of the toroidal comparator.

All results obtained are not restricted to CCCs of the toroidal type, since the coaxial cavity is an element common to all types of CCCs. This is obvious for modifications with telescoped ends. For other modifications a coaxial cavity is formed where the shielded ratio-windings are fed through the SQUID shielding.

To conclude we note that when the relationships between the geometrical shield parameters and the field attenuation are known, it is possible to construct cryo current comparators with a predictable upper limit to the dc error.

The authors wish to thank the Senator für Wirtschaft, Berlin, for financial help and Vacuum-Schmelze, Hanau, for supplying the superconducting materials.

References

1 **Harvey, I.K.** *Rev Sci Instr* **43** (1972) 1626
2 **Grohmann, K., Hahlbohm, H.D., Lubbig, H., Ramin, H.** *PTB-Jahresbericht* **79** (1972) 204
3 **Grohmann, K., Hahlbohm, H.D., Lubbig, H., Ramin, H.** *PTB-Mitteilungen* **83** (1973) 313
4 **Harvey, I.K., Collins, H.C.** *Rev Sci Instr* **44** (1973) 1700
5 **Sullivan, D.B., Dziuba, R.F.** *Rev Sci Instr* **45** (1974) 517
6 **Grohmann, K., Hahlbohm, H.D., Lubbig, H., Ramin, H.** *Cryogenics* **13** (1974) 499
7 **Sullivan, D.B., Dziuba, R.F.** *IEEE Trans Instrum Meas* **IM 23** (1974) 256
8 **Grohmann, K., Hahlbohm, H.D., Lubbig, H., Ramin, H.** *IEEE Trans Instr Meas* **IM 23** (1974) 261
9 **Smythe, W.R.** Static and Dynamic Electricity, 3rd edn (McGraw-Hill, New York)
10 **Dwight, H.B.** *J Math Phys* **27** (1948) 84
11 **Bondarenko, S.I., Vinogradov, S.S., Gogadze, G.A., Perepelkin, S.S., Sheremet, V.I.** *Sov Phys Tech Phys* **19** (1974) 824
12 **Grohmann, K., Hahlbohm, H.D., Hechtfischer, D., Lubbig, H.** (forthcoming)